Structural Engineering and Mechanics, Vol. 23, No. 5 (2006) 487-504
DOI: http://dx.doi.org/10.12989/sem.2006.23.5.487

Analytical *p*-version finite elements and application in analyses of structural collision protection

B. Zhu† and Y. M. Chen‡

Department of Civil Engineering, Zhejiang University, Hangzhou 310027, P. R. China

A. Y. T. Leung‡†

Department of Building and Construction, City University of Hong Kong, Hong Kong, China

(Received October 11, 2005, Accepted March 23, 2006)

Abstract. Several new versatile two-dimensional *p*-version finite elements are developed. The element matrices are integrated analytically to guarantee the accuracy and monotonic convergence of the predicted solutions of the proposed *p*-version elements. The analysis results show that the convergence rate of the present elements is very fast with respect to the number of additional Fourier or polynomial terms in shape functions, and their solutions are much more accurate than those of the linear finite elements for the same number of degrees of freedom. Additionally, the new *p*-version plate elements without the reduced integration can overcome the shear locking problem over the conventional *h*-version elements. Using the proposed *p*-version elements with fast convergent characteristic, the elasto-plastic impact of the structure attached with the absorber is simulated. Good agreement between the simulated and experimental results verifies the present *p*-version finite elements for the analyses of structural dynamic responses and the structural elasto-plastic impact. Further, using the elasto-plastic impact model and the *p*-version finite element method, the absorber of the T structure on the Qiantang River is designed for its collision protection.

Keywords: *p*-version finite elements; structures; impact; experimentation.

1. Introduction

The accuracy of solutions using the finite element method (FEM) may be improved in two ways. The first is the *h*-version to refine the finite element mesh and the second is the *p*-version to increase the order of shape functions for a fixed mesh. The *p*-version elements have several advantages over the *h*-version ones (Zhu 2005): (i) they have better conditioned matrices; (ii) they do not require a change in the mesh to improve the accuracy of solutions of *p*-version elements, which results in that they can be easily used in the adaptive analysis (Papadrakakis and Babilis 1994); (iii) just one *p*-version element can predict accurate solutions for a simple structure; (iv) *p*-

† Lecturer, Corresponding author, E-mail: binzhu@zju.edu.cn
‡ Professor, E-mail: cym@civil.zju.edu.cn
‡† Professor, E-mail: andrew.leung@cityu.edu.hk

version elements tend to give same accurate results with far fewer degrees of freedom (DOFs) than the h-version ones; (v) the p-version elements can overcome the membrane locking, the Poisson locking and the shear locking (Zienkiewicz and Taylor 2000, Tin-Loi and Ngo 2003, Cote and Charron 2001, Dalenbring and Zdunek 2005).

In the last decade, it is very popular to use the Legendre orthogonal polynomials or trigonometric functions as shape functions of p-version elements, and they are named polynomial p-version elements and Fourier p-elements, respectively. Most of studies pay attention to the development of rectangular or skew p-version elements (Bardell 1991, 1992, Beslin and Nicolas 1997, Houmat 2001); however the versatile triangular or arbitrary quadrilateral p-version elements have larger range of application. The existing triangular p-element (Houmat 2000) cannot be integrated analytically and error from the numerical integration will be introduced. The problem becomes obvious for higher terms oscillating in shape functions (Woo *et al.* 2003). Moreover, the numerical integration will soften the stiffness of the element in general and the monotonic convergence of the predicted natural frequencies cannot be guaranteed (Leung and Zhu 2004a). Fortunately, one can always break a triangle into three trapezoids by drawing three lines parallel to the edges from any point inside the triangle. With analytical integration, both trapezoidal Fourier p-elements (Leung and Zhu 2004c, Leung *et al.* 2004) and trapezoidal polynomial p-version elements can produce very high vibration modes of the polygonal structures accurately. However, the exact integration formulae for the arbitrary quadrilateral Fourier p-element cannot be obtained, but they are available for the arbitrary quadrilateral polynomial p-version elements using Legendre orthogonal polynomials as shape functions.

Various impact models and absorbers have been applied for the protection of highway bridges and the structural over-height collision protection (Davalos *et al.* 2001, Qiao *et al.* 2004). For the impact of the structure attached with an absorber, the analyses will be complex and many DOFs should be involved in the computation if the conventional plastic finite elements are used (Qiao *et al.* 2004). Using the fast convergent p-version finite elements, it is efficient to analyze the impact problem just with simple mesh of the structure. Three new two-dimensional p-version finite elements for beams, plane problems and plates are presented in this paper. Vibration of simply supported square plates and fully clamped polygonal plates are analyzed using the proposed plate elements to examine their shear locking free and efficiency of numerical analyses. Then, the proposed new p-version finite elements are used for the elasto-plastic impact analyses and design of absorbers for structural collision protection. Further, a simple impact experiment is carried out to verify the present p-version finite elements.

2. Development of new *p*-version finite elements

The coordinate transformation for the development of two-dimensional p-version finite elements can refer to (Leung and Zhu 2004c, Leung *et al.* 2004). Their C^0 shape functions are

$$N_i(\xi,\eta) = f_j(\xi)f_k(\eta),\ i = 1, 2, \ldots, (p+2)(q+2) \tag{1}$$

where ξ and η are the two mapped plane coordinates; p and q are numbers of additional terms in $f_j(\xi)$ and $f_k(\eta)$, respectively. The first four shape functions $N_1(\xi,\eta)$~$N_4(\xi,\eta)$ $(p=q=0)$ are usually used in conventional linear finite elements (LFE). For the polynomial p-version elements:

Table 1 Definition of two-dimensional p-version finite elements

Name	Shape	Enriching shape functions	Type
THICK-1 (Leung and Zhu 2004b)	-	Trigonometric functions	Beam element
THICK-1H	-	Legendre orthogonal polynomials	Beam element
TFFE-2D (Leung *et al.* 2004)	Trapezoid	Trigonometric functions	Plane element
QHFE-2D	Quadrilateral	Legendre orthogonal polynomials	Plane element
TFFE-P (Leung and Zhu 2004c)	Trapezoid	Trigonometric functions	Plate element
THFE-P	Trapezoid	Legendre orthogonal polynomials	Plate element
QHFE-P	Quadrilateral	Legendre orthogonal polynomials	Plate element

$$f_1(\zeta) = 0.5(1-\zeta), \quad f_2(\zeta) = 0.5(1+\zeta), \quad f_m(\zeta) = \sum_{l}^{m/2} \frac{(-1)^l (2m-2k-5)!!}{2^k k!(m-2k-1)!}\zeta^{m-2k-1} \tag{2}$$

But for the Fourier p-elements:

$$f_1(\zeta) = 0.5(1-\zeta), \quad f_2(\zeta) = 0.5(1+\zeta), \quad f_m(\zeta) = \sin[\pi(m-2)(1+\zeta)/2] \tag{3}$$

In Eqs. (2) and (3), $\zeta = \xi$ or η; $j!! = j(j-2)\ldots 2$ or 1 with $0!! = (-1)!! = 1$; $m = 3, 4, \ldots, p+2$ ($\zeta = \xi$) or 3, 4,..., $q+2$ ($\zeta = \eta$); $m/2$ denotes its own integral part. The additional shape functions with hierarchical polynomials or trigonometric functions lead to zero displacements at each corner node. With these enriching functions, the additional DOFs appear along the four edges and in the interior of the element. The DOFs of the four corner nodes are represented by j, $k \le 2$; the DOFs along the four edges are represented if one of j, $k > 2$; and the DOFs in the interior are represented if both of j, $k > 2$.

Leung and Zhu (2004c) and Leung *et al.* (2004) give analytical element matrices of two-dimensional trapezoidal Fourier p-elements. Since there is one pair of opposite edges of two-dimensional trapezoidal elements paralleling to each other, the two planar coordinates in the Jacobian of the elemental area are uncoupled and can be integrated independently. The integrals in element matrices reduces to $\int \eta^k/(A + C\eta)\mathrm{d}\eta$ and $\int \exp(ik\pi\eta)/(A + C\eta)\mathrm{d}\eta$, in which k is an integer, A and C are constants. The former does not require much attention and the latter is equal to $\frac{1}{e}\exp(-ik\beta\pi)\cdot[\mathrm{Ei}(-ik\beta\pi) - \mathrm{Ei}(-ik(1+\beta)\pi)]$ with $\beta = a/e$ and Ei is the exponential integral function. For two-dimensional arbitrary quadrilateral Fourier p-elements, The integrals in element matrices reduces to $\int \exp(ik\pi\eta)/(A + B\xi + C\eta)\mathrm{d}\xi\mathrm{d}\eta$ where B is a constant, and analytical result of this integral is difficult to be obtained. But for the two-dimensional arbitrary quadrilateral polynomial p-version elements, the integrals in element matrices reduces to $\int \xi^i \eta^j/(A + B\xi + C\eta)\mathrm{d}\xi\mathrm{d}\eta$ with i and j are integers, one can easily deduce its analytical formulation if some commercial packages such as *MAPLE*, *MATLAB* and *MATHEMATICA* are used. The definition of two-dimensional p-version finite elements is shown in Table 1. Using the shape functions of Eq. (2), the p-version thick beam element THICK-1 can be changed to polynomial p-version element THICK-1H.

For engineering applications, the internal DOFs and some DOFs not adjacent to other elements can be condensed by the exact dynamic condensation (Leung 1993) before assembling the elements. By this way, the accuracy of solutions can also be guaranteed and the computational efficiency may be further improved. In the assemblage of p-version elements, since there are DOFs along every edge of the element, direction of the edge between adjacent elements should be in the same orientation to ensure the continuity along the edge.

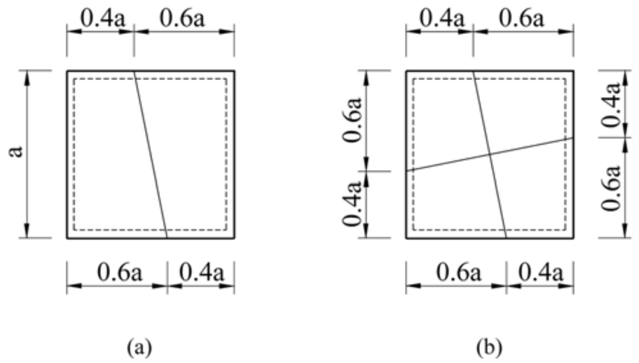

Fig. 1 Mesh for simply supported square plates (a) mesh I, (b) mesh II

3. Numerical studies

3.1 Natural frequencies of simply supported square plates

In this study, to simplify computation and presentation, the number of additional terms in shape functions p is taken the same as q. Analytical solutions are available for the out-of-plane vibration of hard type simply supported (S-S-S-S) square plates (Wang *et al.* 2000). In order to examine the accuracy and the convergence rate of the solutions computed by the p-version finite elements for out-of-plane vibration of plates, S-S-S-S square plates are meshed by two trapezoidal and four quadrilateral elements respectively as shown in Fig. 1. Mesh I is for analyses of TFFE-P and THFE-P, but mesh II is for analyses of QHFE-P. The non-dimensional frequency parameters $\lambda = (\omega a^2/\pi^2)\sqrt{\rho t/D_0}$ are studied, in which ω = circular frequency, ρ = density of the plate, t = thickness of the plate and $D_0 = Et^3/[12(1-\nu^2)]$ with E = Young's modulus and ν = Poisson's ratio. With various numbers of additional terms p in shape functions, the computed frequency parameters λ of the lowest seven modes are shown in Table 2 along with the solutions from the analytical method (Wang *et al.* 2000). From Table 2, it is found that very fast convergence rate is possible with the increasing number of additional terms in shape functions. The results computed by the p-version element with a few Fourier or polynomial terms are in excellent agreement with analytical solutions.

In the analyses of plates by the conventional finite elements, the shear constrain is too strong if the terms in element matrices are fully integrated. So the shear locking problem occurs. This problem can be solved by the reduced integration in h-version finite elements, or introducing p-version finite elements and mixed finite elements. The solutions for the very thin plate with $a/t = 1000$ demonstrate that the polynomial p-version elements THFE-P and QHFE-P are free of the shear locking. But the trapezoidal Fourier p element TFFE-P developed by Leung and Zhu (2004c) cannot overcome the shear locking problem. However, the Fourier p elements are more effective in predicting the medium- and high-frequency modes than the polynomial p-version elements both in precision and in avoiding the ill-conditioning problems (Leung and Zhu 2004c, Leung *et al.* 2004). Comparison with solutions of the linear finite element (LFE) shows that the p-version finite elements produce much more accurate solutions than LFE for the same number of DOFs.

Table 2 Non-dimensional frequency parameters $\lambda = (\omega a^2/\pi^2)\sqrt{\rho t/D_0}$ for out-of-plane vibration of simply supported square plates ($\kappa = 5/6$, $\nu = 0.3$)

a/t	Method	Degrees of freedom	Mode number						
			1	2	3	4	5	6	7
1000	THFE-P ($p = 5$)	197	2.000	5.000	5.046	8.040	10.003	10.403	13.051
	THFE-P ($p = 6$)	272	2.000	5.000	5.005	8.010	10.000	10.170	13.010
	QHFE-P ($p = 4$)	279	2.000	5.000	5.000	8.004	10.005	10.005	13.008
	QHFE-P ($p = 5$)	407	2.000	5.000	5.000	8.000	10.002	10.002	13.004
	QHFE-P ($p = 6$)	559	2.000	5.000	5.000	8.000	10.000	10.000	13.000
	[a]Exact		2.000	5.000	5.000	8.000	10.000	10.000	13.000
	[b]Exact		2.000	5.000	5.000	8.000	10.000	10.000	13.000
10	TFFE-P ($p = 5$)	197	1.934	4.613	4.620	7.085	8.649	8.701	10.843
	TFFE-P ($p = 6$)	272	1.933	4.611	4.617	7.079	8.641	8.648	10.831
	THFE-P ($p = 5$)	197	1.932	4.608	4.615	7.077	8.617	8.730	10.815
	THFE-P ($p = 6$)	272	1.932	4.608	4.608	7.072	8.616	8.669	10.810
	QHFE-P ($p = 4$)	279	1.932	4.608	4.608	7.072	8.620	8.620	10.810
	QHFE-P ($p = 5$)	407	1.932	4.608	4.608	7.072	8.616	8.616	10.810
	QHFE-P ($p = 6$)	559	1.932	4.608	4.608	7.072	8.616	8.616	10.809
	LFE (9 × 9)	224	2.136	5.307	5.352	7.981	10.562	10.590	12.632
	LFE (10 × 10)	279	2.082	5.174	5.174	7.770	10.181	10.181	12.272
	LFE (11 × 11)	340	2.056	5.076	5.076	7.648	9.905	9.905	12.013
	[b]Exact		1.932	4.608	4.608	7.072	8.616	8.616	10.809

[a]Kirchhoff thin plate theory; [b]Mindlin thick plate theory.

3.2 Natural frequencies of fully clamped regular polygonal plates

Vibration of polygonal plates can be analyzed by the point matching method, the collocation method, the Ritz method and so on. The considerable accurate natural frequencies of the polygonal

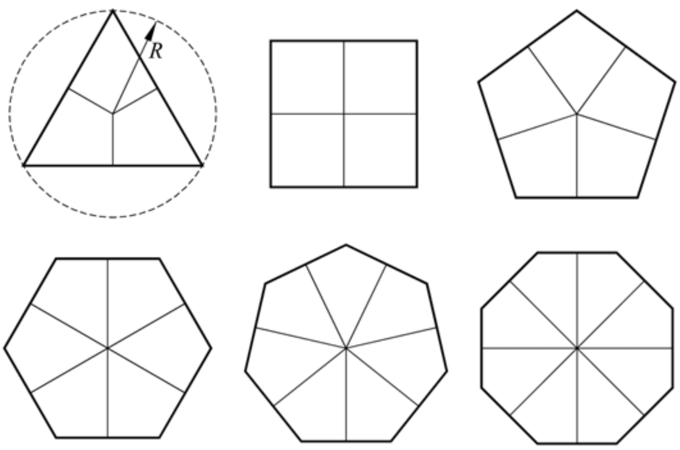

Fig. 2 Meshes for out-of-plane vibration analysis of regular polygonal plates

Table 3 Non-dimensional frequency parameters $\lambda = (4\omega R^2/\pi^2)\sqrt{\rho t/D_0}$ for fully clamped polygonal plates ($\kappa = 5/6$, $\nu = 0.3$, $p = 6$)

Polygon	$2R/t$	Method	Mode number							
			1	2	3	4	5	6	7	8
Triangle	1154.7	QHFE-P	13.38	25.53	25.53	39.89	42.58	42.58	59.22	59.22
		Kitipornchai *et al.* (1993)	13.38	25.53	25.53	39.88	42.58	42.58	-	-
		Irie *et al.* (1978)	13.43	25.81	26.01	42.64	43.17	-	-	-
	11.547	QHFE-P	10.53	17.93	17.93	25.55	26.70	26.70	34.28	34.28
		Kitipornchai *et al.* (1993)	10.51	17.87	17.87	25.48	26.61	26.61	-	-
Square	1414.2	QHFE-P	7.292	14.87	14.87	21.93	26.66	26.79	33.44	33.44
		Liew *et al.* (1993)	7.292	14.87	14.87	21.93	26.66	26.79	33.44	33.44
		Irie *et al.* (1978)	7.317	14.93	14.97	22.11	26.83	27.04	33.6	33.6
	14.142	QHFE-P	6.591	12.57	12.57	17.62	20.76	20.96	25.11	25.11
		Liew *et al.* (1993)	6.591	12.57	12.57	17.62	20.76	20.96	25.11	25.11
Pentagon	1000	QHFE-P	5.803	11.98	11.98	19.37	19.37	22.16	28.60	28.60
		Irie *et al.* (1978)	5.827	12.05	12.08	19.44	19.52	22.20	28.84	28.84
	10	QHFE-P	5.014	9.410	9.410	13.97	13.97	15.61	18.96	18.96
Hexagon	1000	QHFE-P	5.184	10.75	10.75	17.54	17.54	20.01	24.49	26.82
		Liew and Lam (1991)	5.289	10.85	10.85	17.75	17.78	20.23	24.85	27.22
		Irie *et al.* (1978)	5.212	10.85	10.88	17.73	17.75	20.13	24.80	27.10
	10	QHFE-P	4.550	8.624	8.624	12.95	12.95	14.46	16.95	18.08
Heptagon	1000	QHFE-P	4.861	10.10	10.10	16.52	16.52	18.84	24.06	24.06
		Irie *et al.* (1978)	4.884	10.16	10.17	16.62	16.64	18.93	24.21	24.21
	10	QHFE-P	4.305	8.200	8.200	12.37	12.37	13.82	16.72	16.72
Octagon	1000	QHFE-P	4.670	9.706	9.706	15.90	15.90	18.13	23.22	23.22
		Liew and Lam (1991)	4.723	9.880	9.880	16.12	16.12	18.31	23.55	23.55
		Irie *et al.* (1978)	4.696	9.784	9.816	15.99	16.04	18.24	23.40	23.40
	10	QHFE-P	4.159	7.942	7.942	12.01	12.01	13.42	16.28	16.28

plates can also be easily obtained using the p-version finite element method. The p-version meshes of the fully clamped polygonal plates with from three sides to eight sides are shown in Fig. 2, in which R is the common circumscribing radius of the regular polygons. Their frequency parameters λ of the first eight modes are presented in Table 3. A common value of the additional polynomial terms $p = 6$ in QHFE-P is used in the computation. It should be noted that the value of the shear correction factor κ in the literature of Kitipornchai *et al.* (1993) is $\pi^2/12$, and their results are little smaller than the present solutions for the thick triangular plates. Irie (1978) and Liew and Lam (1991) used the Kirchhoff thin plate theory; Liew *et al.* (1993) and Kitipornchai *et al.* (1993) adopted the pb-2 Ritz method which can obtain very accurate solutions for some simple structures. From Table 3, it can be found that the solutions of QHFE-P are in excellent agreement with the results computed by the pb-2 Ritz method, and smaller than those of other methods. The present results of regular polygonal plates may serve as the benchmark data for the development of new methods.

4. Elasto-plastic impact simulation by *p*-version elements

4.1 Experiment installation

A three-dimensional column-plate structure attached with an aluminum absorber subjected to impact deformation is shown in Fig. 3. The geometric size and configuration of elasto-plastic absorbers are shown in Figs. 4 and 5, respectively. A B&K 8202 force transducer is mounted at the head of the impactor. One Kistler 8774 and two Kistler 8776 accelerometers are, respectively, installed on the impactor, at point A and point B of the structure. Some weights are placed on a pendulum to serve as an impactor, and the weight of the impactor can vary as 9.622 kg, 11.622 kg, 13.622 kg, 15.622 kg, 17.622 kg and 19.622 kg. Some associated filters, amplifiers and the data collector used in the experiment are also shown in Fig. 3.

The three-dimensional *p*-version beam element THIN[11] (Leung and Zhu 2004b) and the *p*-version plate element QHFE-P associated with the plane element QHFE-2D are used in the simulation. To save DOFs in the simulation, the absence of torsion DOFs in the beam element is assumed. With the enriching DOFs in these *p*-version elements, the accuracy of the computed vibration modes is

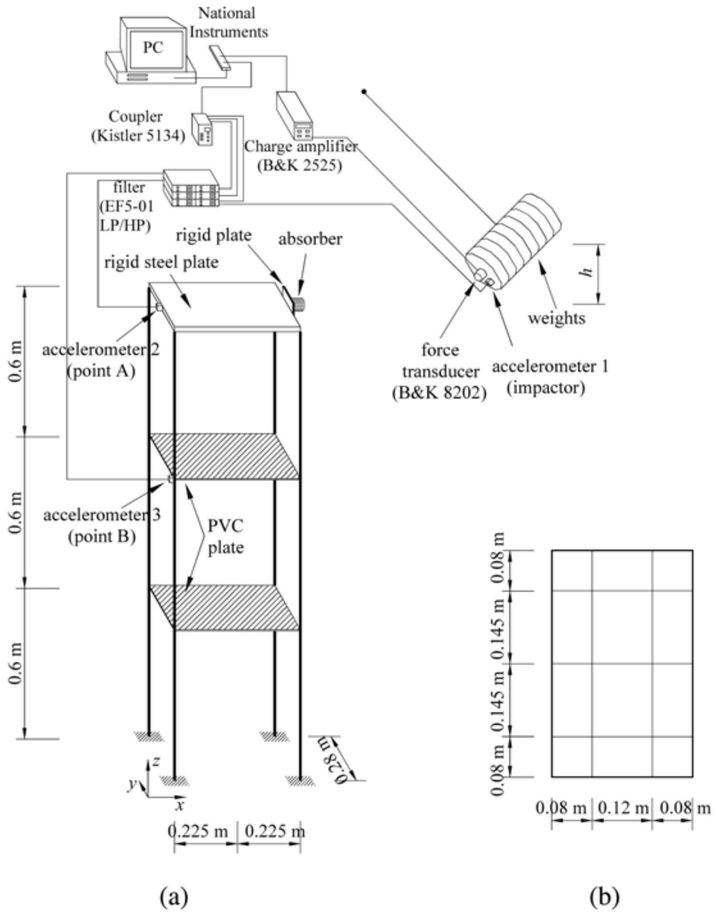

Fig. 3 Experimental setup and analysis model (a) experimental setup, (b) *p*-version mesh of the PVC plate

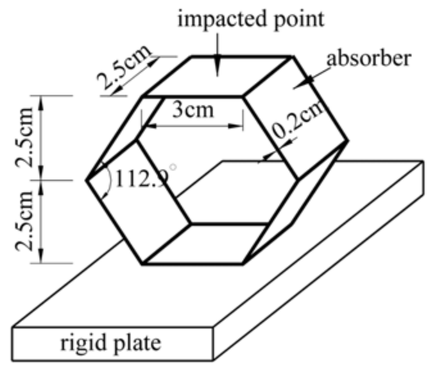

Fig. 4 Geometric size of the aluminum absorber

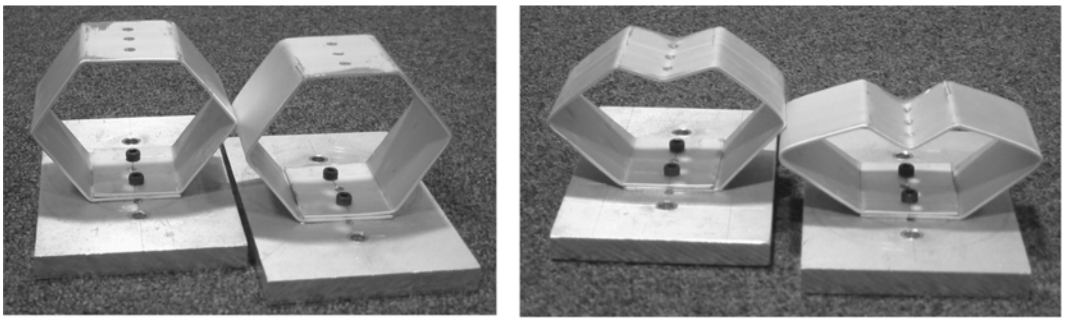

Fig. 5 Configuration of aluminum absorbers (a) before impact, (b) after impact with plastic deformation

Table 4 Properties of materials used for the column-plate structure

Steel columns	Young's modulus E	210×10^9 Pa
	Material density ρ	7800 kg/m
	Length L	0.6 m
	Width b	0.02532 m
	Thickness t	0.00470 m
PVC plates	Young's modulus E	3.7×10^9 Pa
	Material density ρ	1400 kg/m
	Area A	0.45×0.28 m^2
	Thickness t	0.004 m
	shear correction factor κ	5/6
	Poisson's ratio ν	0.3
Rigid steel plate	Mass	25.26 kg

greatly improved. One p-version beam element and twelve p-version plate elements (see Fig. 3(b)) are used for each column and each plate, respectively. Since the top steel plate is rigid, DOFs at the top of the four columns connected to the steel plate are same, and the steel plate is simulated as four masses attached at the top of these four columns. Some physical properties of materials used in

Table 5 Natural frequencies of bending modes of the column-plate structure in the x direction (Hz)

Method	Mode number			
	1	2	3	4
p-version FEM ($p_P = 1$, $p_L = 2$)	0.65	7.08	17.96	23.80
p-version FEM ($p_P = 2$, $p_L = 3$)	0.62	7.02	17.95	19.95
p-version FEM ($p_P = 3$, $p_L = 4$)	0.62	7.00	17.94	18.89
Experiment	0.55	6.80	17.30	18.30

the simulation are listed in Table 4. The convergence rate of the p-version elements for the structure is studied in Table 5 along with the experimental natural frequencies of the first four bending modes in the x direction, in which p_P and p_L are the numbers of additional terms in the shape functions of the plate element and the beam element, respectively. It can be found that the convergence rate of the elements is very fast with respect to the additional terms in shape functions for the first four bending modes of the structure in the x direction. The numbers of additional terms $p_P = 2$ and $p_L = 3$ are used in the impact simulation.

4.2 Damping ratios of the structure

The Rayleigh damping (Clough and Penzien 1993) is adopted in the finite element model of the structure and the damping ratios of the first two modes can be identified using the continuous wavelet transform (CWT) (Zhu 2005, Ruzzene *et al*. 1997). Firstly, the acceleration response of the structure is collected during the free vibration at x direction. With low-pass filtered by 1 Hz and band-pass filtered from 5.8 Hz to 8 Hz, the original signal can be constrained around the first two modes in the x direction, respectively. The free decaying responses of the two filtered signals are shown in Figs. 6(a) and (b). Performing CWT with command *cmor1-1* in *MATLAB* to both signals,

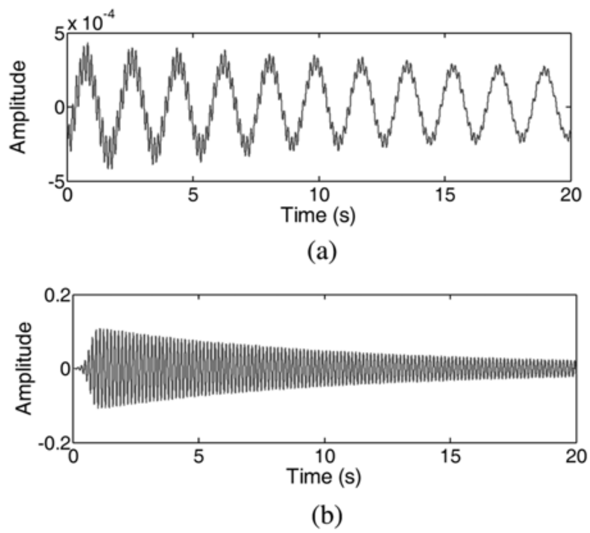

Fig. 6 Free decaying responses of the first two modes (a) first mode, (b) second mode

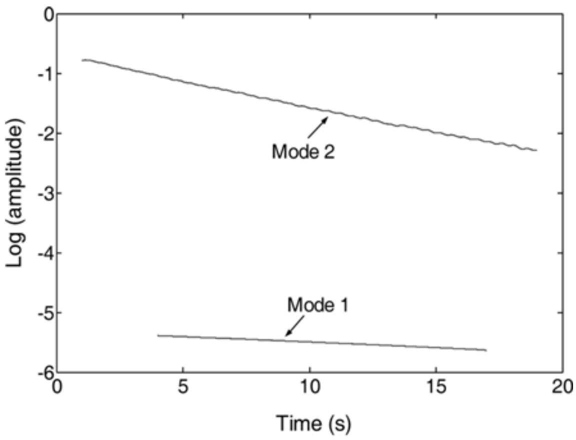

Fig. 7 Peak envelopes of continuous wavelet transformed signals

the peak envelopes of the transformed signals are shown in Fig. 7. Using linear least-square fit, one can calculate the slope S_i of the two lines in Fig. 7 respectively. Then one can obtain the damping ratios of the first two modes by

$$\xi_i = \frac{S_i}{2\pi\omega_{di}} \tag{4}$$

Where ξ_i and ω_{di} are the corresponding damping ratio and damped frequency of the i-th mode. Here damping ratios of first two modes of the x direction are 0.53% and 0.22% respectively, which are used for the Rayleigh damping matrix of the structure. In this paper, responses of the structure are computed by the Newmark linear acceleration method (Clough and Penzien 1993).

4.3 Quasi-static test of the absorber

The quasi-static test of the aluminum absorber is performed by a Lloyd Instruments' LR50KPlus materials testing system. In the test the loading speed is set as 3 mm/min while the loading routes

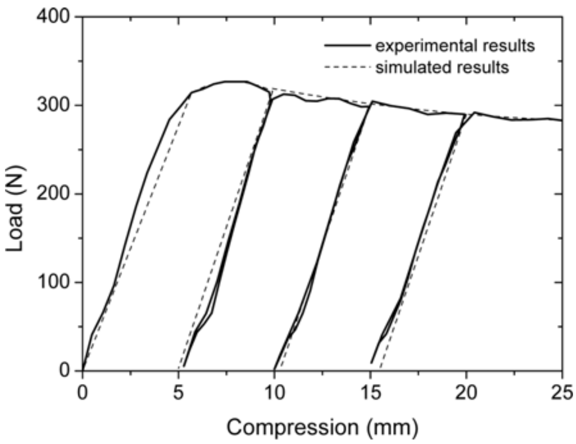

Fig. 8 Experimental and simulated load-deformation relationship of the absorber

are set up as 0→10 mm→0, 0→15 mm→0, 0→20 mm→0 and 0→30 mm, respectively. The force is chosen as the control variable in the test. The experimental results and its simulated curve are plotted in Fig. 8.

4.4 Elasto-plastic impact

Using the simulated load-deformation relationship of the absorber, the elasto-plastic impact process of the structure can be predicted by the elasto-plastic impact model (Zhu 2005, Wu and Yu 2001) and the p-version finite element method. For the presence of elasto-plastic deformation, the impact forces from the simulation and the experiment with different impact energy are compared in Fig. 9. For the case of m = 11.622 kg and h = 0.02 m, in which m and h are the mass and the initial height of the impactor respectively, comparison of the acceleration values at the three accelerometer locations between the simulation and the experiment is carried out in Fig. 10. From Figs. 9 and 10, it can be found that the simulated results are in good agreement with the experimental ones for this three-dimensional structure. The elasto-plastic impact model (Zhu 2005, Wu and Yu 2000) involved in the impact simulation neglects the strain rate effect. Due to the effect of strain rate, the dynamic stress will little larger than the static one (Deshpande and Fleck 2000), as shown in Fig. 9, the

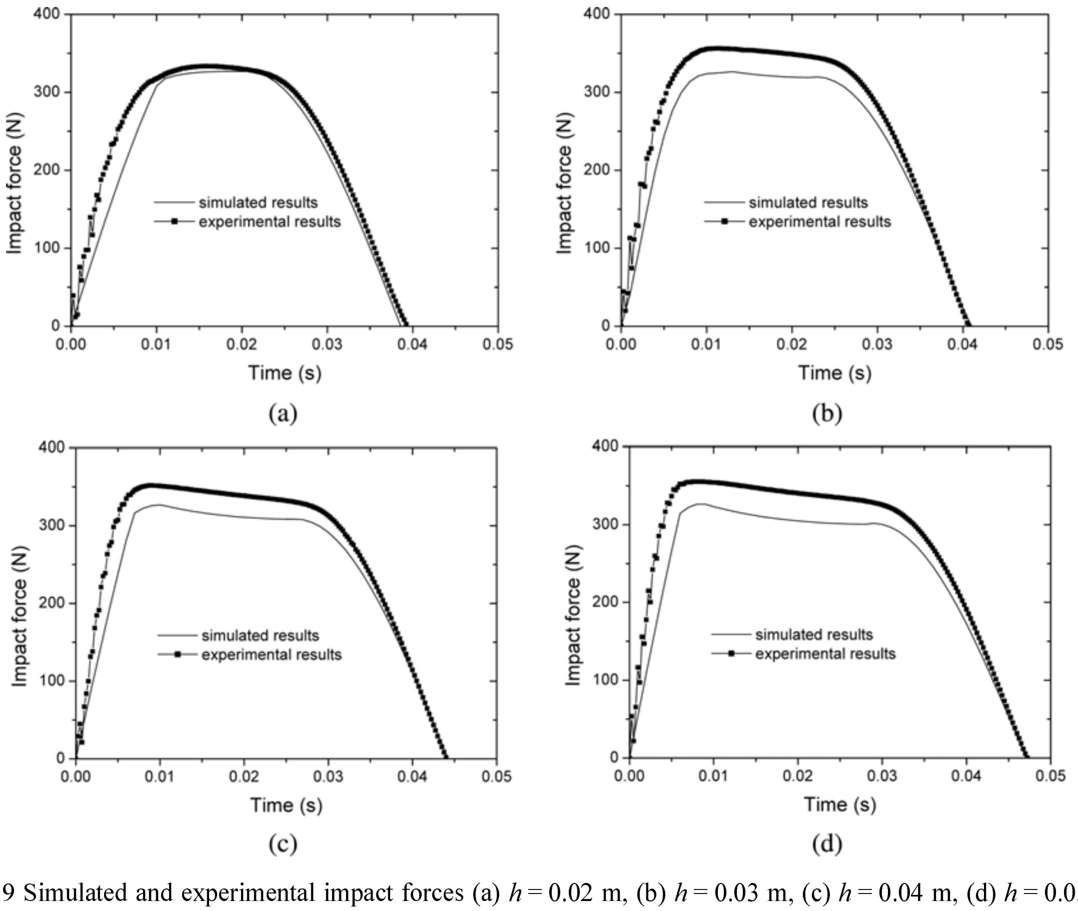

Fig. 9 Simulated and experimental impact forces (a) h = 0.02 m, (b) h = 0.03 m, (c) h = 0.04 m, (d) h = 0.05 m

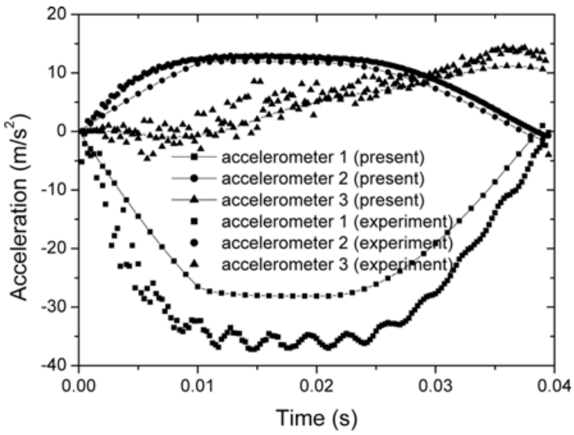

Fig. 10 Comparison of the value of three accelerometers between the simulation and the experiment for the case $m = 11.622$ kg and $h = 0.02$ m

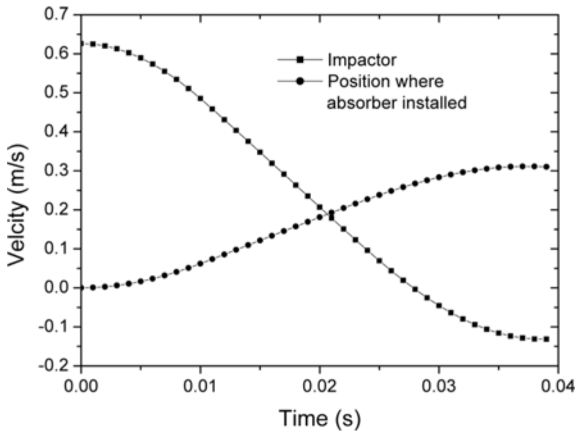

Fig. 11 Velocities of the impactor and the position where absorber installed for the case $m = 11.622$ kg and $h = 0.02$ m

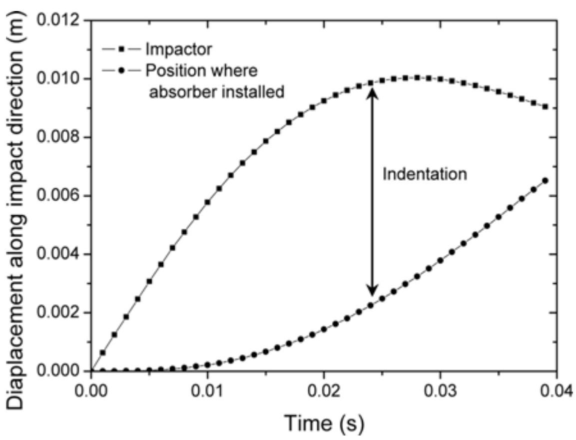

Fig. 12 Displacements of the impactor and the position where absorber installed for the case $m = 11.622$ kg and $h = 0.02$ m

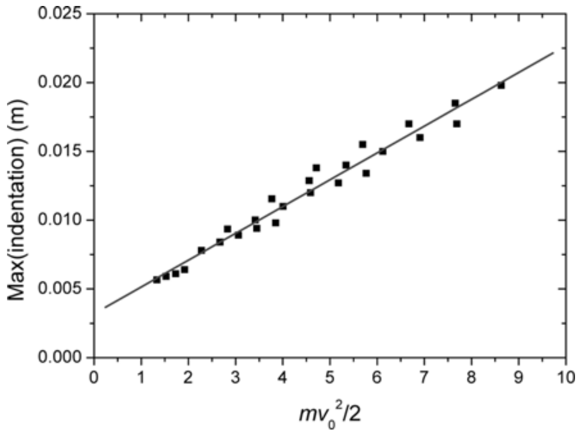

Fig. 13 Maximal indentation of absorbers in the simulation

difference between the simulated and tested impact force increases with the increasing of impact velocities. Further, the tested dynamic responses of the impact system are also little larger than the simulated ones as shown in Fig. 10. The simulated velocities and the displacements of the impactor and the position where the absorber locates on the structure are shown in Figs. 11 and 12, respectively. During the impact process, the velocity of the impactor decreases to zero and then the impactor turns around. The impactor and the absorber depart from each other when the impact force reaches zero, at which the indentation of the absorber is the final plastic deformation after the impact (see Fig. 12). As shown in Fig. 13, the plastic deformation of absorbers is almost linearly related to the impact energy $mv_0^2/2$ in this case where v_0 is the velocity of the impactor just before the impact. The deformation of the absorber during the impact is one of the most important parameters since it determines the size of the absorber for the collision protection.

5. Absorber design for T structure on Qiantang River

A T structure used to weaken the famous Qiantang bore and protect the Qiantang dike is shown in Fig. 14. There are two rows of reinforced concrete piles with length of 11 m embedded in the mucky soil, which are connected to each other (see Fig. 14(a)) by cap beams and collar beams. The piles toward the upstream of the river are numbered as P1-P22.

Since the structure is transversely extended into the river, impact by moving ships on the

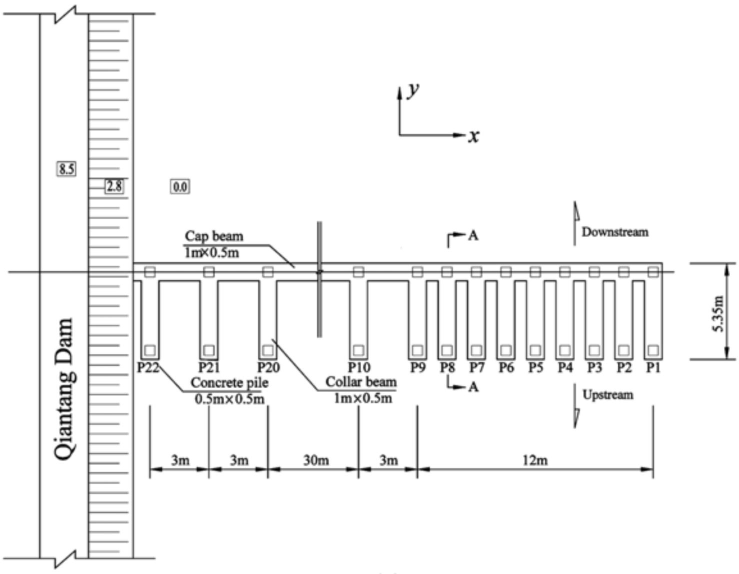

(a)

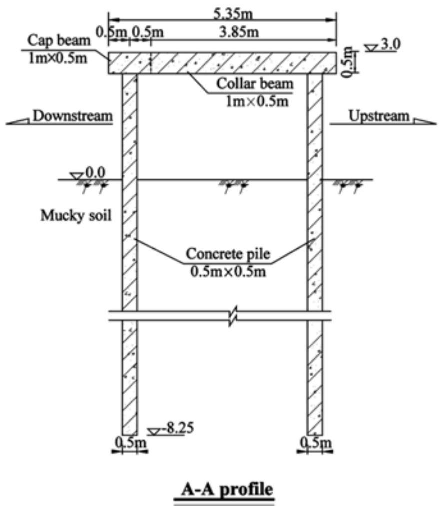

(b)

Fig. 14 T structure on the Qiantang River (a) plane view, (b) cross-section view

Table 6 Physical properties of impact analysis of T structure

T structure	Young's modulus E	30×10^9 Pa
	Material density ρ	2500 kg/m
	Shear correction factor κ	1
	Poisson's ratio ν	0.3
Moving ship	Moving speed	3 m/s
Foundation	Winkler foundation modulus k	2×10^6 Pa
	Shear foundation modulus k_G	2.5×10^7 N

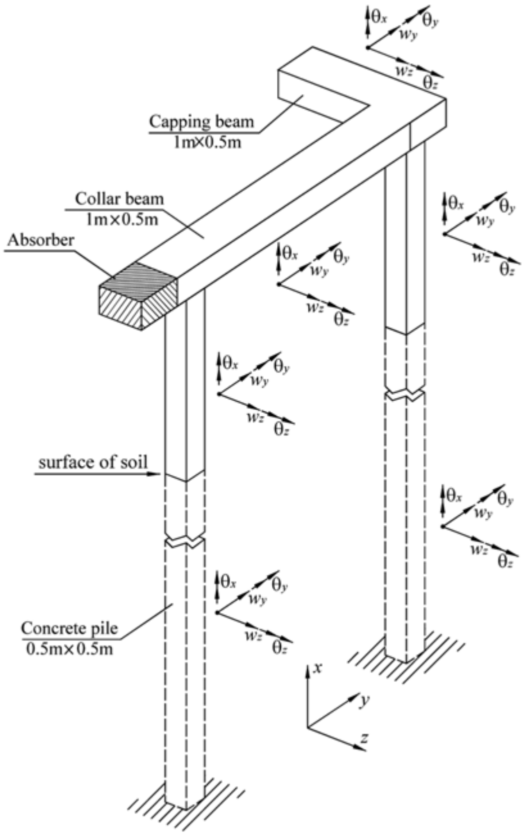

Fig. 15 p-version finite element model of the substructure

Qiantang River is common. Some physical properties of the structure and the moving ship are shown in Table 6. Just parts of DOFs of the structure are taken into account to simplify the computation (see Fig. 15). The polynomial p-version thick beam element THICK-1H is used in the computation. There is one element for each cap beam and each collar beam respectively, but two elements for each pile. The element for the part of the pile in soil is also THICK-1H but rests on two-parameter foundation. Convergence study of the p-version elements is shown in Table 7, in which p is the common number of additional polynomial terms involved in shape functions for all elements. It can be found that the convergence rate of the elements is very fast with respect to the

Table 7 Natural frequencies of the T structure (Hz)

HFEM	Mode							
	1	2	3	4	5	6	7	8
$p=2$	5.519	7.587	12.08	16.19	18.08	18.74	19.11	19.35
$p=3$	5.518	7.584	12.08	15.95	17.52	18.02	18.30	18.47
$p=4$	5.515	7.582	12.07	15.95	17.52	18.02	18.30	18.47
$p=5$	5.515	7.582	12.07	15.95	17.52	18.02	18.30	18.47
$p=6$	5.515	7.582	12.07	15.95	17.52	18.02	18.30	18.47

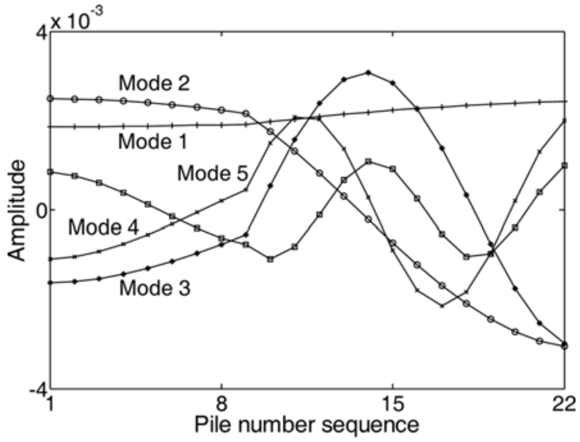

Fig. 16 Transverse vibration mode shapes at the top of piles P1~P22 for the first five modes of the T structure

value of p and solutions with $p=4$ are accurate enough for the computation. The first five transverse vibration mode shapes at the top of piles P1-P22 are plotted in Fig. 16.

In view of large impact energy of the moving ship, the cellular reinforced concrete absorber is a good choice to protect this structure from the ship collision (Zhu 2005). The load-deformation relationship of the concrete absorber can be simplified as $F = F_0x/D_0$ $(0 \le x \le D_0)$ and $F = \alpha x + F_0(x > D_0)$ where F(N) and x(m) are the applied load and the compression of the absorber, respectively; F_0, D_0 and α are constants. With this bilinear load-deformation relationship of the absorber and the p-version FEM, the optimal strength and size of the absorber can be computed as follows.

Various F_0, $D_0 = 0.73377 \times 10^{-3}$ m and $\alpha = 78533$ are used in the simulation to study the effect of strength of the absorber. Shown in Fig. 14 the right part of the structure tends to be impacted more than the left one, and it is clear that responses of the structure will be largest if the top of the pile P1 is impacted. Thus, only the transverse impact at the top of the pile P1 is analyzed herein, and the appropriate concrete absorber is selected for the protection of this location. The moving ship is from the upstream of the river and with the speed of $v_0 = 3$ m/s. The maximal indentation of the absorber decreases as the increase of strength of the absorber as shown in Fig. 17. Actually, the strength of the absorber determines the impact force. Hence, with the increasing strength of absorbers, responses of the structure decrease as shown in Fig. 18. The absorber with small strength can much smooth the impact force as well as responses of the structure, but deformation of the absorber

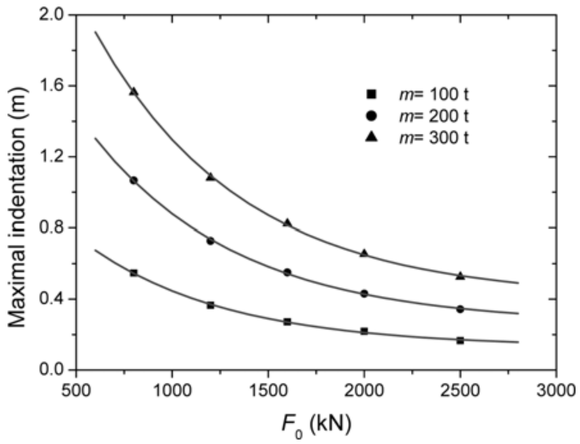

Fig. 17 Maximal indentation of the absorber with different strength

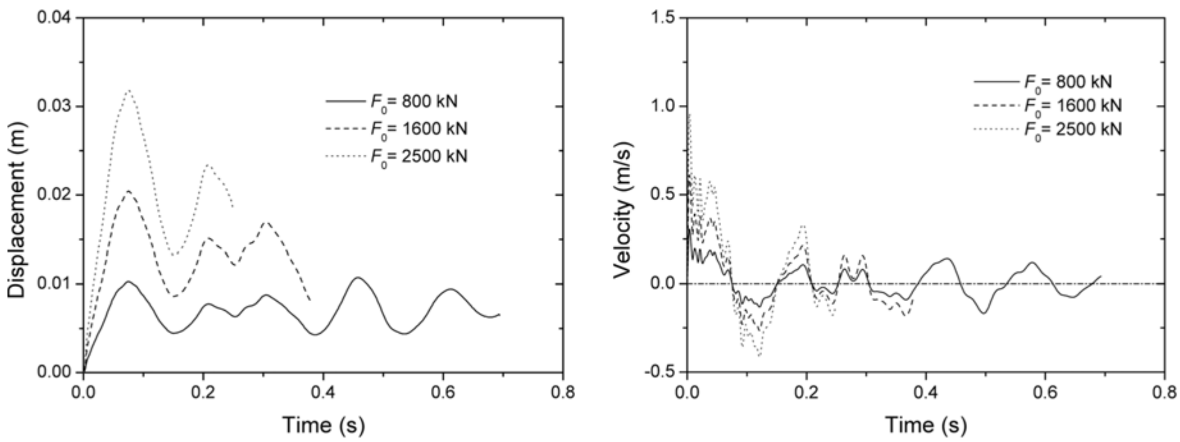

(a) (b)

Fig. 18 Reponses at impacted position on structure for impactor with mass of 200 t (a) displacement response, (b) velocity response

during the impact will be large. In the design of absorber for structural collision protection, strength of the structure should be checked according to responses of the structure during the impact and using some related design codes in civil engineering, then the appropriate strength and size of the absorber can be selected based on the simulated results. For example, for the case of $m = 200$ t and maximal (indentation) = 1.0 m, the value of F_0 will be about 750 kN (see Fig. 17), if the strength of the T structure during the impact is satisfied. By this way, the optimal absorber can be selected for the collision protection of the T structure.

6. Conclusions

Element matrices of the proposed two-dimensional p-version finite elements are integrated analytically to guarantee the accuracy and monotonic convergence of solutions. The present *p*-version plate elements without the reduced integration overcome the shear locking problem over some conventional *h*-version elements. Computational results show that the convergence rate of the present elements is very fast with respect to the number of additional terms in shape functions. Even with very simple mesh of the structure, the present elements can also obtain very accurate solutions which are much more accurate than those of the linear finite elements for the same number of DOFs.

Since there are many time steps in the computation of time-domain responses using the linear acceleration method, much computational time will be saved if less DOFs are used. In general, the *p*-version finite elements can produce more accurate solutions than the *h*-version ones, so the *p*-version FEM is a superior method for the computation of structural dynamic responses. The present *p*-version finite elements are used for the simulation of elasto-plastic impact of a three-dimensional structure attached with an absorber. Good agreement between the simulated and experimental results verifies the proposed *p*-version finite elements for the structural vibration analyses. Using the present *p*-version finite elements, the absorber for the collision protection of the T structure on the Qiantang River is designed. For the impact of the structure attached with an absorber, usually, only the absorber deforms plastically. The analyses will be complex and many DOFs should be involved in the computation to satisfy the accuracy requirement if the conventional plastic finite elements are used. With the present simple impact model and fast convergent *p*-version elements, the analyses of this type of impact are simple and accurate enough for engineering applications. But if there is plastic deformation in the impactor or the structure, plastic *p*-version finite elements should also be considered. The *p*-version FEM associated with the simple impact model is an attractive method for the impact analyses of the structure attached with the absorber in engineering applications.

References

Bardell, N.S. (1991), "Free vibration analysis of a flat plate using the hierarchical finite element method", *J. Sound Vib.*, **151**(2), 263-289.

Bardell, N.S. (1992), "The free vibration of skew plates using the hierarchical finite element method", *Comput. Struct.*, **45**(5-6), 841-874.

Beslin, O. and Nicolas, J. (1997), "Hierarchical functions set for predicting very high order plate bending modes with any boundary conditions", *J. Sound Vib.*, **202**(5), 633-655.

Clough, R.W. and Penzien, J. (1993), *Dynamics of Structures*, 2nd Edition, McGraw-Hill, New York, U.S.A.

Cote, A. and Charron, F. (2001), "On the selection of *p*-version shape functions for plate vibration problems", *Comput. Struct.*, **79**, 119-130.

Davalos, J.F., Qiao, P.Z., Xu, X.F., Robinson, J. and Barth, K.E. (2001), "Modeling and characterization of fiber-reinforced plastic honeycomb sandwich panels for highway bridge applications", *Comp. Struct.*, **52**, 441-452.

Dalenbring, M. and Zdunek, A. (2005), "On the use of three-dimensinal *h*- and *p*-version finite elements in solving vibration response problems", *J. Sound Vib.*, **288**, 907-929.

Deshpande, V.S. and Fleck, N.A. (2000), "High strain rate compressive behaviour of aluminium alloy foams", *Int. J. Impact Eng.*, **24**, 277-298.

Houmat, A. (2001), "A sector Fourier *p*-element applied to free vibration analysis of sectorial plates", *J. Sound Vib.*, **243**(2), 269-282.

Houmat, A. (2000), "A triangular Fourier *p*-element for the analysis of membrane vibrations", *J. Sound Vib.*, **230**(1), 31-43.

Irie, T., Yamada, G. and Narita, Y. (1978), "Free vibration of clamped polygonal plates", *Bulletin of the JSME*, **21**, 1696-1702.

Kitipornchai, A., Liew, K.M., Xiang, Y. and Wang, C.M. (1993), "Free flexural vibration of triangular Mindlin plates", *Int. J. Mech. Sci.*, **35**(2), 89-102.

Leung, A.Y.T. (1993), *Dynamic Stiffness and Substructures*, Springer-Verlag, London, U.K.

Leung, A.Y.T. and Zhu, B. (2004a), "Comments on "Free vibration of skew Mindlin plates by *p*-version of FEM"", *J. Sound Vib.*, **278**(3), 699-703.

Leung, A.Y.T. and Zhu, B. (2004b), "Fourier *p*-elements for curved beam vibrations", *Thin-Walled Structures*, **42**(1), 39-57.

Leung, A.Y.T. and Zhu, B. (2004c), "Transverse vibration of thick polygonal plates using analytically integrated trapezoidal Fourier *p*-element", *Comput. Struct.*, **82**(2-3), 109-119.

Leung, A.Y.T., Zhu, B., Zheng, J.J. and Yang, H. (2004), "Analytic trapezoidal Fourier *p*-element for vibrating plane problems", *J. Sound Vib.*, **271**(1-2), 67-81.

Liew, K.M. and Lam, K.Y. (1991), "A set of orthogonal plate functions for flexural vibration of regular polygonal plates", *J. Vib. Acoustics*, **113**(3), 182-186.

Liew, K.M., Xiang, Y. and Kitipornchai, S. (1993), "Transverse vibration of thick rectangular plates-I. Comprehensive sets of boundary conditions", *Comput. Struct.*, **49**(1), 1-29.

Papadrakakis, M. and Babilis, G.P. (1994), "Solution techniques for the *p*-version of the adaptive finite element method", *Int. J. Numer. Meth. Eng.*, **37**, 1413-1431.

Qiao, P.Z., Yang, M.J. and Mosallam, A.S. (2004), "Impact analysis of I-Lam sandwich system for over-height collision protection of highway bridges", *Eng. Struct.*, **26**, 1003-1012.

Ruzzene, M., Fasana, A., Garibaldi, L. and Piombo, B. (1997), "Natural frequencies and damping identification using wavelet transform: Application to real data", *Mechanical Systems and Signal Processing*, **11**(2), 207-218.

Tin-Loi, F. and Ngo, N.S. (2003), "Performance of the *p*-version finite element method for limit analysis", *Int. J. Mech. Sci.*, **45**, 1149-1166.

Wang, C.M., Reddy, J.N. and Lee, K.H. (2000), *Shear Deformable Beams and Plates*, Elsevier, Oxford, U.K.

Woo, K.S., Hong, C.H., Basu, P.K. and Seo, C.G. (2003), "Free vibration of skew Mindlin plates by *p*-version of F.E.M", *J. Sound Vib.*, **268**(4), 637-656.

Wu, K.Q. and Yu, T.X. (2001), "Simple dynamic models of elastic-plastic structures under impact", *Int. J. Impact Eng.*, **25**, 735-754.

Zhu, B. (2005), "*p*-version finite elements and applications in structural impact and damage detection", Ph. D Thesis, City University of Hong Kong, Hong Kong, China.

Zienkiewicz, O.C. and Taylor, R.L. (2000), *The Finite Element Method.* 5th Edition, Vol. 1, Butterworth-Heinemann, Oxford, 276-304.